Supporting Information for

Thermoelectrically driven photocurrent generation in femtosecond laser patterned graphene junctions

Aleksei V. Emelianov,[1,*] Dmitry Kireev,[2] Andreas Offenhäusser,[2] Nerea Otero,[3] Pablo M. Romero,[3] and Ivan I. Bobrinetskiy[1]

[1]*National Research University of Electronic Technology, Zelenograd 124498, Russia*

[2]*Institute of Complex Systems - Bioelectronics (ICS-8), Forschungszentrum Jülich, Jülich 52425, Germany*

[3]*Laser Applications Centre, AIMEN, Porriño 36410, Spain*

**E-mail: emmsowton@gmail.com*

Table of Contents

1. The experimental setup for graphene FETs processing and graphene functionalization

We used 280-fs pulsed laser to functionalize GFETs with oxygen species in normal conditions. The pulse peak energy was set to 2 nJ and the number of pulses per μm^2 was varied through scanning speed from 3300 to 50000 pulses per μm^2 (from 150 down to 10 μm/s).

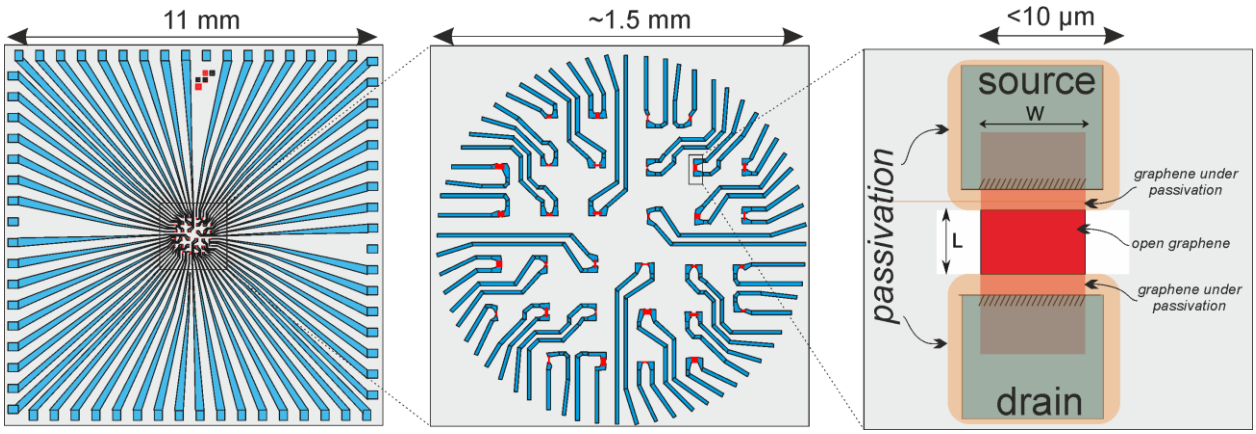

Figure S1. The geometry of fabricated GFETs with different channel width and length, Au/Ti (100/10 nm) electrodes and polyimide layer passivation. Metallic feedlines are shown in blue, graphene in red and passivation in dark orange. The passivation is important to ensure chip's integrity as well as the absence of electrolyte leakage currents through the experiments.

We processed twenty-two GFETs (the geometry is shown in Figure S1) with different fs-laser speed across the channel via setup shown in Figure S2. The main parameters for twelve structures are shown in Table S1. Additional eight structures were processed with the same parameters as GFET4-GFET11, and two structures were treated with a photon flux higher than 15×10^{25} photons/(s m^2), which led to total oxidation of the graphene channel.

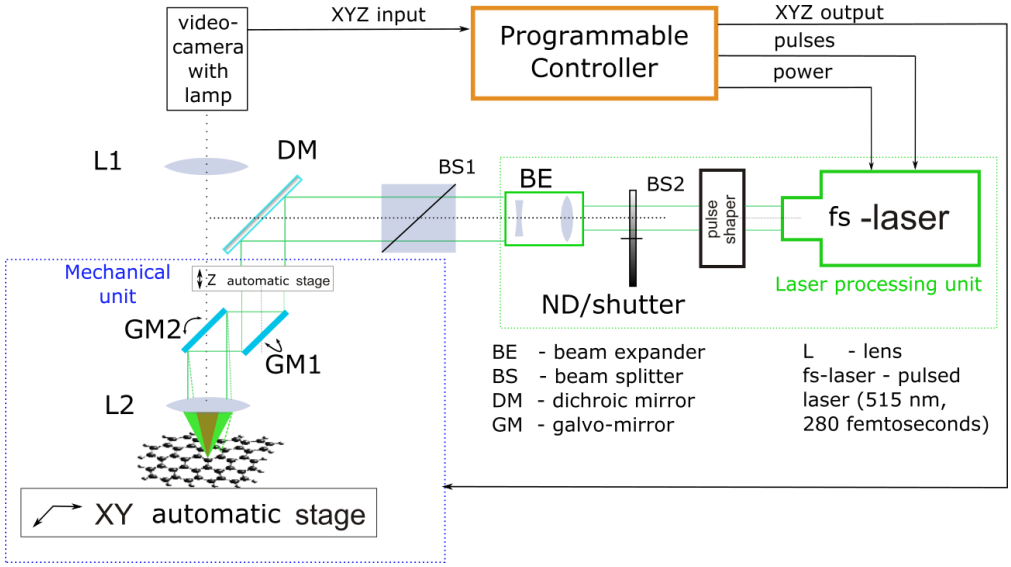

Figure S2. The scheme of the experimental setup for GFET treatment.

In our research, we used the laser emitting parameter "photon flux" to express the dosage of fs-laser irradiation. To find photon flux we need to calculate the energy of a single photon and the number of photons per pulse. The energy of a single photon for our system is equal to:

$$E\ (1\ \text{photon}) = \frac{hc}{\lambda} = 3.86 \times 10^{-19}\ \text{J} \qquad (1)$$

Then we can find the number of photons per pulse by the following equation:

$$\#\ \text{of photons} = \frac{\text{E (1 pulse)}}{\text{E (1 photon)}} = 5.04 \times 10^9\ \text{photons} \qquad (2)$$

We know the number of pulses per μm^2 from scanning speed, the repetition rate (was set at 500 kHz) and the diameter of the beam spot (~2μm). Thus, we can find the photon flux following the next expression:

$$\text{Photon flux} = \frac{\#\ \text{of photons} \times \#\ \text{of pulses per}\ \mu m^2}{\text{time of treatment}} \qquad (3)$$

We found that the peak energy fluence, calculated for multiple fs-laser pulses and resulted in functionalization of single-layer graphene, exceeds the peak energy fluence needed to ablate graphene by a single pulse. Therefore, we can conclude that the ultrafast physical and chemical processes are different for single and multiple pulsed fs-laser treatment.

Table S1. Parameters of laser processing and properties change in GFETs.

Structure	Photon flux, 10^{25} photons/(s m^2)	G band shift, cm^{-1}	Initial I_D/I_G	I_D/I_G after laser treatment	Initial I_{ON}/I_{OFF}	I_{ON}/I_{OFF} after laser treatment	V_{CNP} shift (liquid gate), mV	R change, %
GFET-1	1.68	0	0.06	0.05	2.2	2.3	10	3
GFET-2	2.10	0	0.04	0.05	1.8	1.8	15	2
GFET-3	2.52	1	0.14	0.31	2.5	2.8	50	16
GFET-4	2.80	3	0.04	0.13	2.4	3.5	70	5
GFET-5	3.15	4	0.05	0.27	3.7	3.8	95	25
GFET-6	3.60	3	0.05	0.16	2.4	3.6	90	2
GFET-7	3.88	6	0.04	0.21	1.1	1.8	100	120
GFET-8	4.58	8	0.07	1.05	2.2	4.9	160	100
GFET-9	6.30	5	0.07	0.78	1.3	4.5	80	120
GFET-10	7.20	6	0.08	0.92	3.5	6	130	200
GFET-11	12.60	7	0.1	1.04	4.5	9	150	1000
GFET-12	14.00	10	0.09	1.26	2.6	3	-60	4000

Table S2. Data calculated from Raman spectra of pristine and treated GFET-8.

GFET-8	D band, cm^{-1}	G band, cm^{-1}	2D band, cm^{-1}	I_D/I_G	I_{2D}/I_G	$I_D/I_{D'}$	FWHM (G)	FWHM (2D)
pristine	1348	1594	2689	0.07	0.78	3.5	7	30
functionalized	1348	1598	2694	1.05	0.69	13	12	33

2. STM measurements of pristine and functionalized CVD graphene

We performed STM measurements using Pt/Rh tip on 1x1 cm Si/SiO_2 substrate with CVD grown single-layer graphene. Graphene lattice was treated with the same parameters as GFET-8. After laser modification graphene was flattened by contact AFM measurement. We measured the I-V curves through a single point spectroscopy under normal conditions (Figure S3).

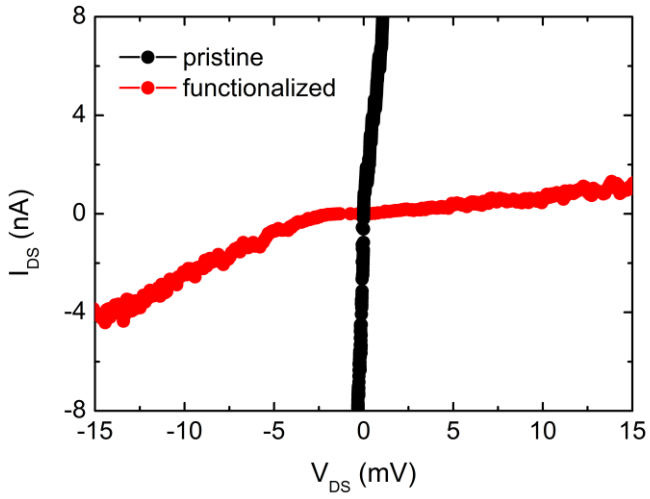

Figure S3. STM spectroscopy measurements of pristine and functionalized graphene.

3. Mobility calculations for GFET

We calculated the mobility for GFET-11 with graphene channel width and length of 2 and 18 μm, respectively.

The equation to estimate μ is as follows:

$$I_{DS} = \frac{W}{L} \cdot C_{ox} \cdot \mu \cdot (V_{GS} - V_{CNP}) \cdot V_{DS}$$

In order to estimate the mobility, especially far from the CNP, it is possible to simplify the calculations as follows:

$$g = \frac{dI_{DS}}{dV_{GS}}; \qquad \mu = \frac{L}{W} \cdot \frac{g}{C_{ox} V_{DS}}$$

Where g is the transconductance calculated deriving the conductance curve. The mobility can be simply calculated from transconductace, assuming C_{ox} = 2-3 μF/cm^2 for liquid-gated devices.[S1,S2] However, in a more complicated case, the C_{ox} is also dependent on (V_{GS}-V_{CNP}), and therefore μ is a function of V_{GS}.[S3]

Yet, as in accordance to above papers, we will calculate only max values of mobility, which are far (100-150 mV) from the Dirac point, and the solution, used for the electrochemical gating is 1x PBS, we use a value of 2 μF/cm^2.

Table S3. Calculated maximal hole and electron mobilities for GFET-11 before and after fs-laser modification.

GFET 11	Before laser treatment	After laser treatment
Max hole mobility, cm^2/(V s)	1400	150-170
Max electron mobility, cm^2/(V s)	1000	80-100

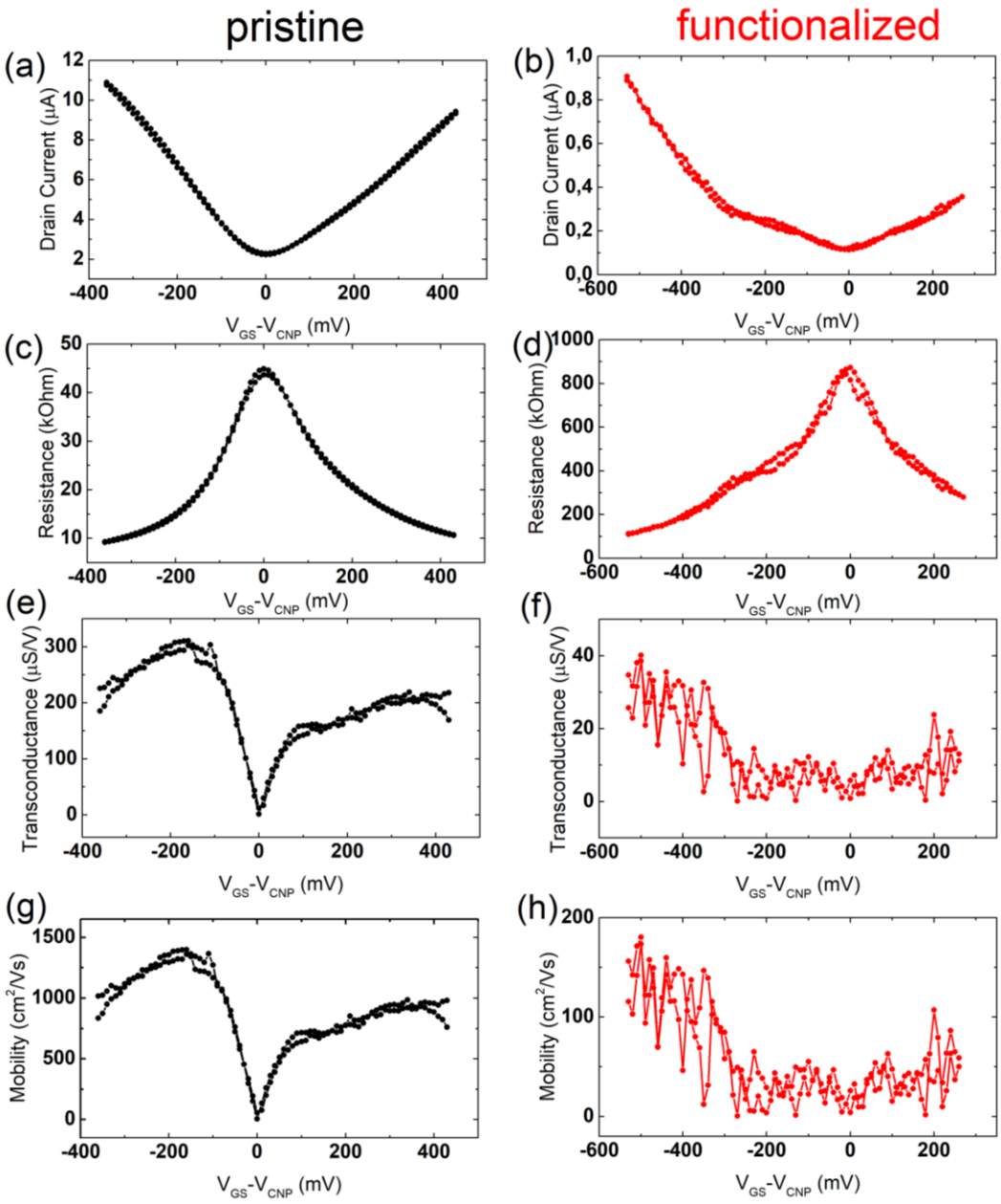

Figure S4. I_{DS}-V_{GS} curves (a-b), R-V_{GS} curves (c-d), transconductance plots (e-f) and mobility values (g-h) for pristine and functionalized GFET-11.

4. Comparison of the photoresponsivity, NEP, and LDR of graphene photodetectors

In Table S4 we compare the main photodetector parameters, such as noise level, responsivity, and LDR of our functionalized devices with literature.

Table S4. Comparison of the main parameters of graphene photodetectors.

active layer	modification method	wavelength, nm	thermoelectric power, μW/K	P_{sat}*, kW/cm^2	NEP**, kW/cm^2	LDR***, dB	responsitivity, mA/W	reference
exfoliated BLG/SLG	pristine	635	6	0.7	-	-	0.17	[S4]
exfoliated SLG	asymmetric contacts	1550	NA	51	10	7.5	6.1	[S5]
CVD SLG	interfacial doping by silane SAM	532	60	120	3.3	15	0.65	[S6]
exfoliated SLG	CW laser	532	-	-	-	-	0.2	[S7]
FLG- $FeCl_3$	CW laser	473	NA	$>10^4$	4	44	0.05	[S8]
exfoliated SLG	annealed	690	NA	2	-	-	0.25	[S9]
exfoliated SLG	Ar^+ plasma	514.5	20	$>10^4$	-	-	0.09	[S10]
exfoliated SLG	Ar^+ plasma	535	-	0.4	-	-	37	[S11]
CVD SLG	**Fs-laser**	**532**	**60**	**$>10^4$**	**6**	**42**	**100**	**this work**

*Power density at which saturation of photocurrent is observed

**Noise Equivalent Power

***Linear Dynamic Range

5. Photocurrent dependence on graphene channel width

We found that the photoresponse highly depends on the GFET channel width (Figure S5). The narrower the graphene channel, the higher the photocurrent signal. We associate this effect with contact/body area relation.

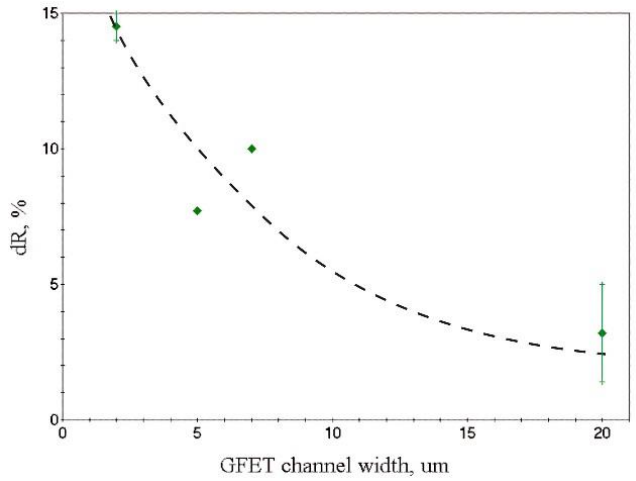

Figure S5. The change of GFETs-8-11 resistance upon fs-laser irradiation with 1×10^{25} photons/(s m^2) versus channel width.

6. Photocurrent generation by fs-laser pulses

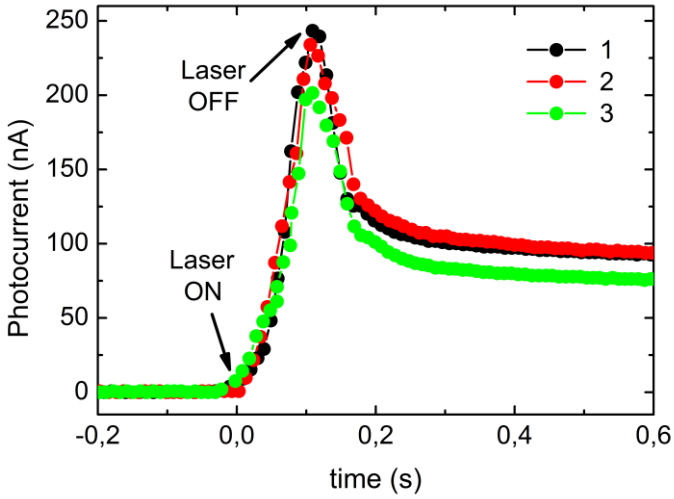

Figure S6. The photocurrent generation process in functionalized GFET-8 upon fs-laser irradiation with 1×10^{25} photons/(s m^2). Graphene channel was scanned with speed of 70 μm/s. The time between experiments (1, 2 and 3) was ~ 30 sec. V_{DS} was set at 5 mV.

7. Pristine graphene photoresponse upon CW laser irradiation

We measured output and transfer I-V curves of pristine GFET upon CW laser irradiation and without light. The results show almost no evidence of photocurrent generation and no prominent V_{CNP} shift upon 532 nm laser irradiation compared with functionalized GFETs.

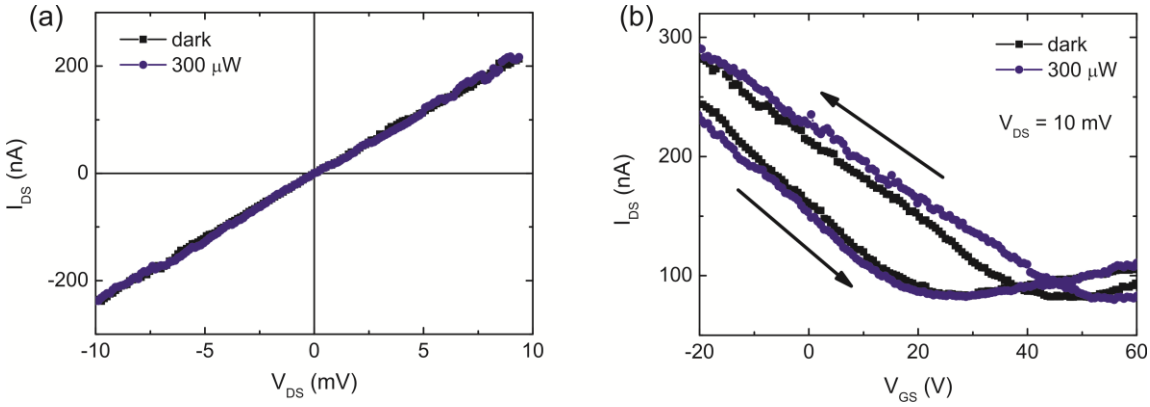

Figure S7. (a) Output I-V curves for pristine single-layer graphene channel in dark and upon 532 nm laser irradiation. (b) Transfer I-V curves for pristine graphene channel in dark and upon 532 nm laser irradiation.

8. Photocurrent generation upon continuous laser irradiation

The relaxation times of excited charge carriers after CW laser irradiation are rather high, but an increase of V_{DS} should empty trap states faster.

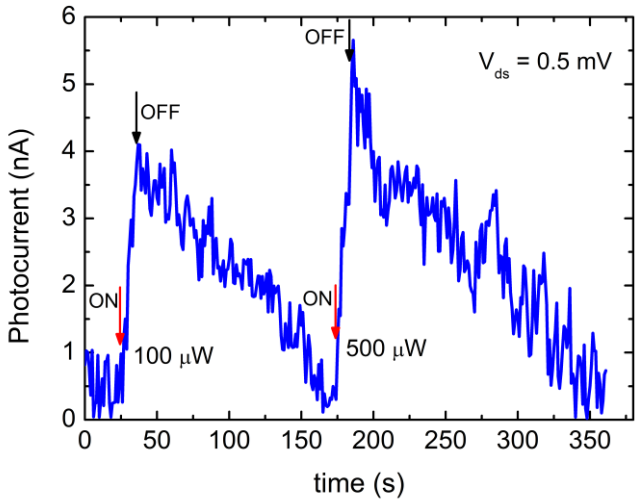

Figure S8. The relaxation time of charge carriers measured upon CW 532 nm laser irradiation. The red and black arrows show the time points of turning on and turning off of the laser beam, respectively.

References

(S1) Hess, L. H.; Hauf, M. V.; Seifert, M.; Speck, F.; Seyller, T.; Stutzmann, M.; Sharp, I. D.; Garrido, J. A. High-Transconductance Graphene Solution-Gated Field Effect Transistors. *Appl. Phys. Lett.* **2011**, *99* (3), 033503.

(S2) Hess, L. H.; Seifert, M.; Garrido, J. A. Graphene Transistors for Bioelectronics. *Proc. IEEE* **2013,** *101* (7), 1780-1792.

(S3) Kireev, D.; Brambach, M.; Seyock, S.; Maybeck, V.; Fu, W. Y.; Wolfrum, B.; Offenhausser, A. Graphene Transistors for Interfacing with Cells: Towards a Deeper Understanding of Liquid Gating and Sensitivity. *Sci. Rep.* **2017,** *7*, 6658.

(S4) Xu, X. D.; Gabor, N. M.; Alden, J. S.; van der Zande, A. M.; McEuen, P. L. Photo-Thermoelectric Effect at a Graphene Interface Junction. *Nano Lett.* **2010,** *10* (2), 562-566.

(S5) Mueller, T.; Xia, F.; Avouris, P. Graphene Photodetectors for High-Speed Optical Communications. *Nat. Photonics*, **2010**, *4*, 297-301.

(S6) Wang, S.; Sekine, Y.; Suzuki, S.; Maeda, F.; Hibino, H. Photocurrent Generation of a Single-Gate Graphene p–n Junction Fabricated by Interfacial Modification. *Nanotechnology*, **2015**, *26*, 385203.

(S7) Wang, W. H.; Nan, H. Y.; Liu, Q.; Liang, Z.; Yu, Z. H.; Liu, F. Y.; Hu, W. D.; Zhang, W.; Wang, X. R.; Ni, Z. H. Distinct Photoresponse in Graphene Induced by Laser Irradiation. *Appl. Phys. Lett.* **2015,** *106* (2), 021121.

(S8) Sanctis, A. De; Jones, G. F.; Wehenkel D. J.; Bezares, F.; Koppens, F. H. L.; Craciun, M. F.; Russo, S. Extraordinary Linear Dynamic Range in Laser-Defined Functionalized Graphene Photodetectors. *Sci. Adv.* **2017**, *3*, e1602617.

(S9) Freitag, M.; Low, T.; Xia, F. N.; Avouris, P. Photoconductivity of Biased Graphene. *Nature Photon.* **2013,** *7* (1), 53-59.

(S10) Du, R. X.; Wang, W. H.; Du, J. X.; Guo, X. T.; Liu, E.; Bing, D.; Bai, J. Photoresponse in Graphene Induced by Defect Engineering. *Appl. Phys. Express* **2016,** *9* (11), 115101.

(S11) Thiyagarajan, K.; Saravanakumar, B.; Kim, S. J. Gate-Tunable Photoresponse of Defective Graphene: from Ultraviolet to Visible. *ACS Appl. Mater. Interfaces* **2015,** *7* (4), 2171-2177.